Cold Regions Science and Technology 220 (2024) 104134

Contents lists available at ScienceDirect

Cold Regions Science and Technology

journal homepage: www.elsevier.com/locate/coldregions

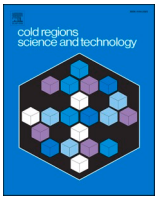

A new interpolation method to resolve under-sampling of UAV-lidar snow depth observations in coniferous forests

Vasana Dharmadasa [a,b,c,*], Christophe Kinnard [a,b,c], Michel Baraër [d]

[a] Department of Environmental Sciences, University of Québec at Trois-Rivières, QC G8Z 4M3, Canada
[b] Center for Northern Studies (CEN), Québec City, QC GV1 0A6, Canada
[c] Research Centre for Watershed-Aquatic Ecosystem Interactions (RIVE), University of Québec at Trois-Rivières, Trois-Rivières, QC G8Z 4M3, Canada
[d] Department of Construction Engineering, École de technologie supérieure, Montréal, QC H3C 1K3, Canada

ARTICLE INFO

Keywords:
UAV-lidar
Under-sampling
Interpolation
Systematic trends
Forested sites
Snow distribution

ABSTRACT

Obtaining accurate snow depth estimates under dense canopies using airborne lidar (light detection and ranging) techniques is challenging due to the under-sampling of ground and snow surfaces. Existing interpolation techniques do not adequately address this problem and they often result in an overestimation of under-canopy snow depths. To address this issue, we introduce and evaluate a new interpolation method that incorporates intra-canopy snow depth variability to provide more accurate estimations at unsampled locations. Four interpolation methods were tested, considering systematic trends (landscape trend, canopy vs. gap trend, and intra-canopy trend) along with spatial interpolation of the residuals. Our results show that spatial interpolation methods without consideration of trends are sufficient to capture and reconstruct the small-scale variability of snow depths below a separation distance of 1 m between sampled and unsampled locations, (i.e., ground surface point density > 1 pt. m^{-2}). However, beyond a separation distance of 2.5–3 m (point density < 0.33–0.40 pt. m^{-2}), spatial interpolation based on proximity alone becomes unreliable because point separation becomes larger than the snow depth spatial correlation scale. Within these limiting distances, the method that incorporates trends along with spatial interpolation techniques can resolve the small-scale variability and thereby reduce the likely overestimation of snow depths under the canopy.

1. Introduction

Airborne (both piloted and unpiloted) lidar (light detection and ranging) scanning has been increasingly used in recent years to monitor snowpacks in forested environments due to its strong penetration ability through the forest canopy to detect underlying snow cover and ground (Hopkinson et al., 2004; Morsdorf et al., 2006; Hopkinson et al., 2012b; Deems et al., 2013; Harpold et al., 2014; Zheng et al., 2016; Currier and Lundquist, 2018; Zheng et al., 2018; Mazzotti et al., 2019; Harder et al., 2020; Jacobs et al., 2021; Dharmadasa et al., 2022; Koutantou et al., 2022; Dharmadasa et al., 2023). Among the airborne techniques, interest in the use of unmanned aerial vehicle (UAV) laser scanning for small scale high-resolution mapping has been on the rise. This is due to its capability to produce dense, high-quality point clouds with reduced occlusion in forested areas compared with airborne laser scanning (ALS) (Broxton et al., 2015; Pajares, 2015; Glira et al., 2016; Michele et al., 2016; Painter et al., 2016; Currier and Lundquist, 2018; Mazzotti et al., 2019; Harder et al., 2020). In forested environments, ground returns point density depends on forest cover type, understory vegetation, laser spot size, laser pulse rate, and the scan angle of the laser sensor (Deems et al., 2013). As such, dense canopies, especially snow-laden conifer canopies, pose challenges for under-canopy snow depth detection by reflecting and attenuating larger amounts of lidar pulses and thereby preventing laser shots from reaching the ground/snow surface (Varhola et al., 2010; Hopkinson et al., 2012b; Harpold et al., 2014; Tinkham et al., 2014; Broxton et al., 2015; Zheng et al., 2016; Mazzotti et al., 2019; Zheng et al., 2019; Jacobs et al., 2021; Koutantou et al., 2022; Dharmadasa et al., 2023). Consequently, this under-sampling of snow under canopies introduces errors upon averaging or interpolating snow depth points to a different resolution (Tinkham et al., 2014; Zheng et al., 2016). Since forest openings (gaps) generally accumulate more snow than under canopies and have higher lidar point densities (Hopkinson et al., 2012a; Broxton et al., 2015; Revuelto et al., 2015; Hojatimalekshah et al., 2021), aggregating or interpolating point snow depths can

* Corresponding author at: Department of Environmental Sciences, University of Québec at Trois-Rivières, QC G8Z 4M3, Canada.
E-mail address: vasana.sandamali.dharmadasa@uqtr.ca (V. Dharmadasa).

https://doi.org/10.1016/j.coldregions.2024.104134
Received 24 April 2023; Received in revised form 17 January 2024; Accepted 22 January 2024
Available online 23 January 2024

results in an overestimation bias in the resulting averaged snow depth map (Zheng et al., 2016). For example, in a dense mixed-conifer forest in the southern Sierra Nevada, Zheng et al. (2016) found that 28% of the area had no lidar returns, which resulted in at least a 10 cm overestimation error in average snow depth for the whole area when using snow depths in the open area as estimates of under-canopy snow depths. In addition, along with the influence of coniferous tree canopy interception, sublimation, longwave emittance, and unloading of snow from the canopy lead to relatively lower snow depths closer to the tree trunk and a gradual increase in snow depth up to a distance coinciding with the canopy crown (Pomeroy and Dion, 1996; Musselman et al., 2008; Revuelto et al., 2015; Zheng et al., 2019), resulting in significant, but somewhat predictable, intra-canopy variability of snow depths in coniferous forests. Existing interpolation techniques such as inverse distance weighting (Burrough, 1986; Guo et al., 2010; Michele et al., 2016), geostatistical methods (Isaaks and Srivastava, 1989; Guo et al., 2010; Mazzotti et al., 2019; Koutantou et al., 2022), regression and tree-based methods (Winstral et al., 2002; Jost et al., 2007; López-Moreno et al., 2010; Lehning et al., 2011; Revuelto et al., 2014; Zheng et al., 2018), or a combination of these methods (Erxleben et al., 2002) do not fully address the aforementioned caveats. Koutantou et al. (2022) emphasized the need for a more sophisticated gap-filling algorithm to avoid likely overestimation of under-sampled under-canopy snow depths. In this study, we address and explore the problem of biased snow depth distributions due to under-canopy under-sampling in coniferous environments, and introduce and evaluate a new interpolation method that incorporates the intra-canopy snow depth variability and thus providing more accurate estimations at unsampled locations. This method seeks to decompose and model the overall lidar snow depth variability into systematic components (landscape trend, preferential accumulation in gaps, intra-canopy variability) and remaining stochastic variability, for an optimal interpolation of lidar snow depths in coniferous forests and more accurate landscape-wide snow depth distribution estimates. To determine the optimal method, four methods were assessed, which combined the systematic trends and spatial interpolation of residuals. We hypothesize that spatial interpolation methods that only exploit the spatial correlation of available lidar snow depths will be insufficient to fill the gaps in coniferous forests, where systematic variations in snow depth occur over beneath and among tree canopies.

2. Study area

The study site, Forêt Montmorency (hereafter Montmorency) is a dense boreal forest with a mean canopy density of 60–80%, located north on the Canadian Shield (47.3°N, 71.1°W) in southern Québec, eastern Canada (Fig. 1). Dominant tree species of the site are balsam fir (*Abies balsamea*), black spruce (*Picea mariana*), and white spruce (*Picea glauca*). The maximum canopy radius was found to be 7 m in Montmorency area (Dharmadasa et al., 2023). One of the characteristics of the area is forest gaps associated with clear-cutting and regeneration practices (Québec Ministry of Forests, Wildlife, and Parks (MFFP)). Lidar

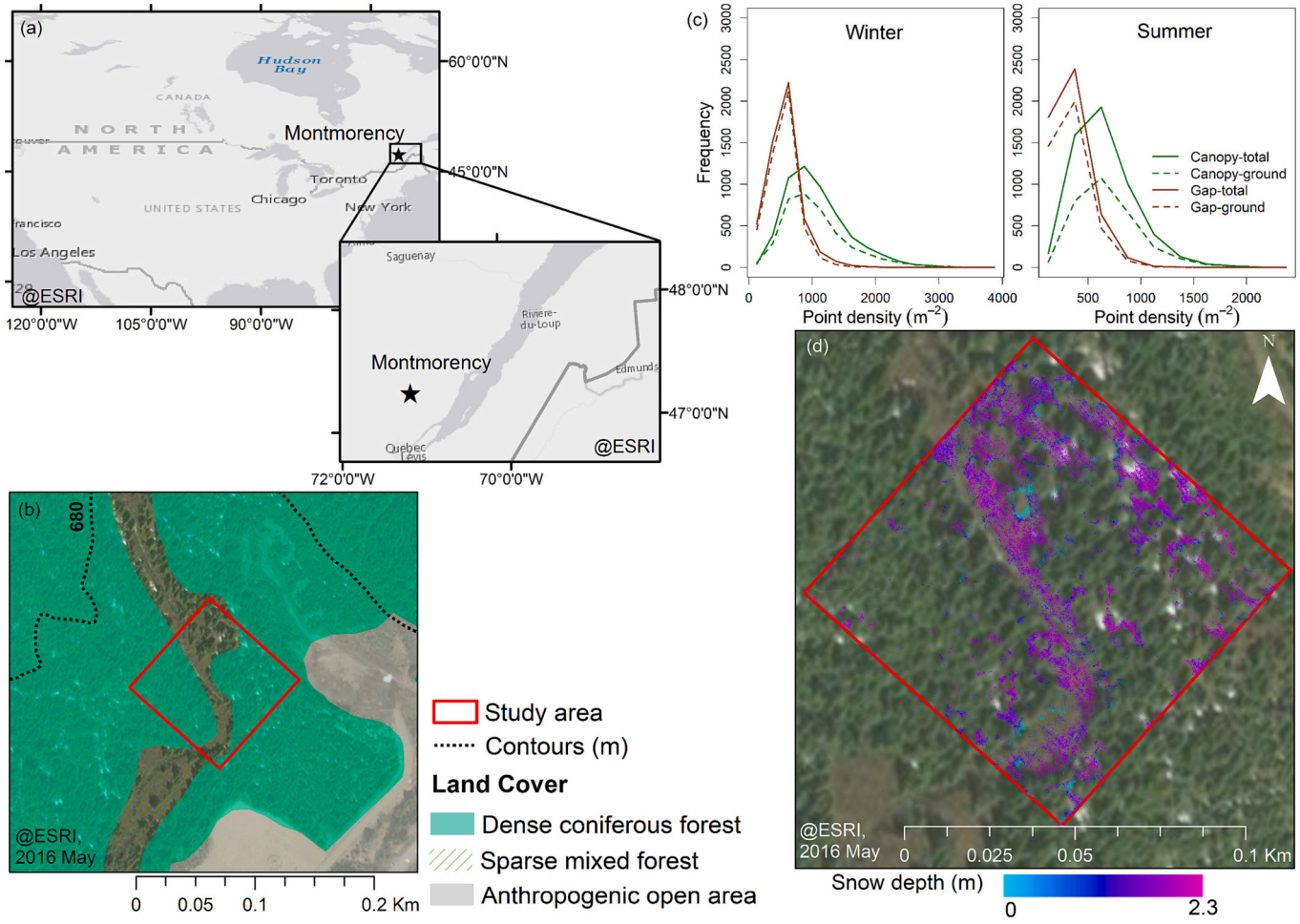

Fig. 1. (a) Location of the Montmorency site, (b) 100 × 100 study area (demarcated in red) with land uses (adapted from MFFP) superimposed on satellite image, (c) frequency of total vs. ground lidar returns under canopies and gaps in the study area for winter and summer surveys, and (d) raw snow depth map of the study area at 0.1 m resolution (see Methods). (For interpretation of the references to colour in this figure legend, the reader is referred to the web version of this article.)

data acquisition of the site was conducted in winter for the snow-on surface (29 March 2019) and early summer 2019 for the snow-off surface (13 June 2019) with a GeoMMS system mounted onto a DJI M600 Pro UAV platform. The VLP-16 lidar sensor on board the GeoMMS system uses 16 infra-red lasers with a wavelength of 905 nm, each pulsating at 18.08 kHz and retrieves measurements up to 600,000 points/s in dual return mode, with a 3 cm precision at 50 m above ground level (AGL) (VelodyneLiDAR, 2018). Post processing of lidar data was done in the Geodetics proprietary software LiDARTool (Geodetics Inc, 2019) with PPK (Post process kinematic) correction based on a local GNSS base station deployed at each survey site. A 100 × 100 m representative area (Fig. 1) from the broader survey conducted in Montmorency by Dharmadasa et al. (2022) was used in this study. More details on data acquisition and equipment specifications are described in Dharmadasa et al. (2022). As observed on Fig. 1 and in the field campaign also, the sparse mixed forest area in Fig. 1 is mostly composed of forest gaps.

3. Methods

The post-processed and classified lidar point clouds obtained from Dharmadasa et al. (2022) were used to produce the snow depth distribution map used in this study. A detailed presentation of lidar point cloud processing is given by Dharmadasa et al. (2022). The workflow presented in Fig. 2 depicts the sequence of steps that were used to produce the snow depths maps, extract tree canopies, and develop the new snow depth interpolation methods.

3.1. Raw snow depth map

A snow depth map (hereafter raw snow depth map) was produced at 0.1 m grid resolution (Fig. 1d), following the same procedure described in Dharmadasa et al. (2022) and Dharmadasa et al. (2023), to account for the variability of snow depth within the canopy; i.e., bare surface points were aggregated to a grid resolution of 0.1 m using the binning method in Global Mapper (Blue Marble Geographics, 2020). Rather than interpolating, this method uses the average of the bare surface points within a grid cell, hence preserving the observation gaps in the data.

3.2. Segmentation of individual trees

We developed a canopy height model (CHM) at 0.5 m resolution and identified the treetops in the winter point cloud normalized by bare surface point elevations in the R package lidR (Roussel et al., 2020; Roussel et al., 2022). CHM at 0.5 m resolution was found to capture well the treetops and extract canopies. A lower grid size would risk introducing topographic variability in the CHM, leading to complications in identifying treetops and delineating canopy polygons. A local maximum was detected to identify treetops using flexible window sizes ranging from 3 to 5 m. We used the region-growing algorithm developed by Dalponte and Coomes (2016) for tree segmentation on our data. Fig. 3 shows the treetops and tree polygons (canopy crowns) identified by the tree segmentation algorithm. Note that, at times, for a cluster of trees with interlocking crowns, only a single treetop was identified. Zheng et al. (2018) found that the canopy surrounding within an 8 m radius of a tree has a stronger effect on the snow accumulation on the ground, so that a clustered canopy has a stronger effect on snow depths than a single tree canopy. It was also confirmed during field works that these clusters of trees act as a single unit which intercepts snow as a whole and reduces snow accumulation underneath. Therefore, identifying a single treetop for a cluster of interlocking trees was deemed acceptable for the purpose of the study. After the segmentation of individual trees, all snow depth grid cells within the tree polygons were defined as “under-canopy”, whereas the snow depth grid cells outside the tree polygons were defined as “forest gaps”. A similar approach for tree segmentation was

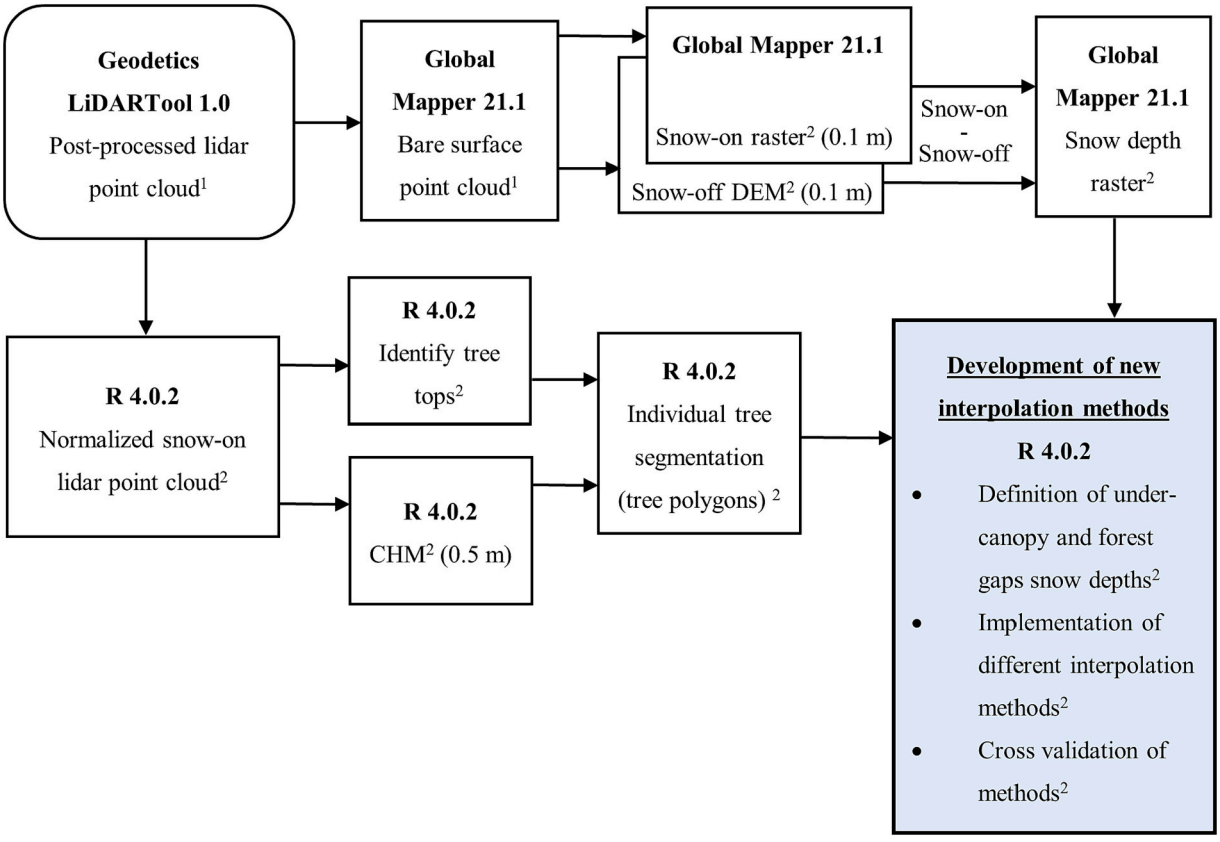

Fig. 2. Workflow adopted for the study. Each box shows the software used (bold) with the corresponding end product. [1] adapted from Dharmadasa et al. (2022). [2] developed for this study. DEM = Digital elevation model and CHM = Canopy height model.

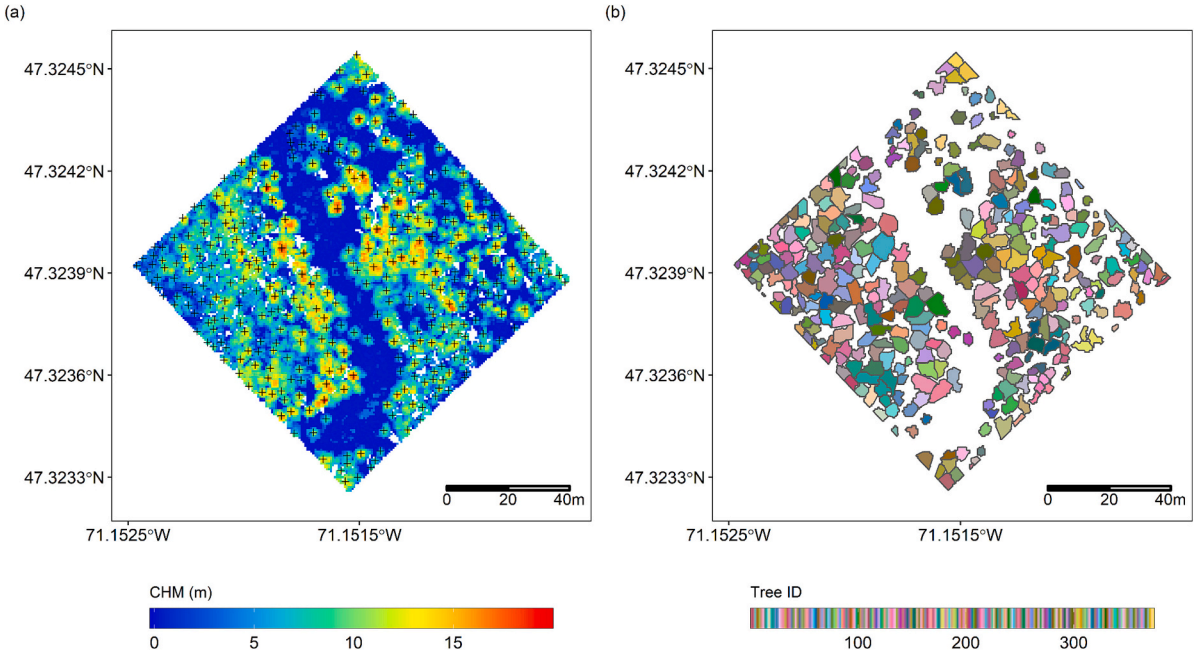

Fig. 3. Results of tree segmentation. (a) treetops plotted as crosses (+) over the canopy height model (CHM), (b) tree polygons identified for each treetop.

previously used by Hojatimalekshah et al. (2021) on terrestrial laser scanning data collected across Grand Mesa, Colorado, USA.

3.3. Development of new interpolation methods

We implemented four different interpolation methods on raw snow depth grid cells. The methods differed in which of the systematic trends (landscape trend, canopy vs. gap trend, and intra-canopy trend) were considered, or not, during the interpolation process. Method 1 only considered the landscape trend of the snow depths; method 2 considered the landscape trend and the canopy vs. gap trend; Method 3 considered the landscape trend and the intra-canopy trend in snow depths; finally, method 4 considered all systematic trends (landscape trend, canopy vs. gap trend and intra-canopy trend). For each method, the systematic trends were modelled and removed (Table 1), and the residuals were spatially interpolated using either local-inverse distance weighting (IDW) or the geostatistical ordinary kriging (OK) method, that are the most commonly used spatial interpolation techniques. With IDW, the weight of each point is inversely proportional to the distance between the samples (Burrough, 1986). With OK, a semi-variogram that summarizes the spatial structure of the snow depth grid cells is used to calculate the weighting factor that corresponds to each point to estimate snow depth at unsampled locations (Isaaks and Srivastava, 1989). Both methods were tested separately for the interpolation of residuals. In addition, spatial interpolation of raw snow depth maps using OK and IDW approaches was used as a reference to show the effect of modelling and including systematic trends. All analyses were done in R 4.0.2. Fig. 4 summaries the methods interrelations and Table 1 outlines the different systematic trends considered in this study.

3.3.1. Interpolation method 1

In method 1, we first removed the landscape trend in raw snow depth grid cells by fitting a second-order polynomial trend surface (Table 1; Eq. 1) using the spatial package in R (Venables and Ripley, 2002). Then, the snow depth residuals (raw snow depth – landscape trend: 'residual 1' on Fig. 4) were spatially interpolated using OK and IDW. The landscape trend is then added back to the interpolated residuals to obtain the estimated snow depths in unsampled areas.

Table 1
Overview of different systematic trends. The SD term in each trend equation is the snow depth modelled by the trends, and not the final interpolated snow depths.

Trend	Description	Equation
Landscape	Second order polynomial trend surface.	$SD = a\,x^2 + 2b\,xy + c\,y^2 + 2d\,xz + 2e\,yz + f\,z^2$ Eq. 1 *SD* is the raw snow depth, *x*, *y*, *z* are cartesian coordinates and *a*, *b*, *c*, *d*, *e*, *f* are coefficients.
Canopy vs. gap	Average of the detrended snow depths under canopies and gaps.	$SD_{gap} = \overline{Residual\ 1_{gap}}$ Eq. 2 $SD_{canopy} = \overline{Residual\ 1_{canopy}}$ Eq. 3 *Residual 1* is obtained by subtracting the snow landscape trend from the raw snow depths.
Intra-canopy	Weighted second order polynomial regression function with scaled distance (0 to 1) from the tree stem to tree canopy edge as predictor and tree height as interactive term. The weights correct for the decreasing point density towards the tree stem and are calculated with a kernel density function with a bandwidth of 0.1 of scaled distance.	$SD = \left(a\,dis + b\,dis^2 + c\,H + d(H\,dis) + e\right)$ Eq. 4 *dis* is scaled distance, *H* is tree height, *a*, *b*, *c*, *d* are coefficients, and *e* is the intercept. *SD* is either the residual of the landscape trend in method 3 (Residual 1) or those from the canopy vs. gap trend in method 4 (Residual 2).

3.3.2. Interpolation method 2

In method 2, the detrended snow depth data from method 1 (residual 1) was used to calculate the canopy vs. gap trend. For this, the average snow depth under-canopy and within forest gaps were calculated and subtracted from residual 1 (Table 1; Eq. 2 and 3), yielding the 2nd-level

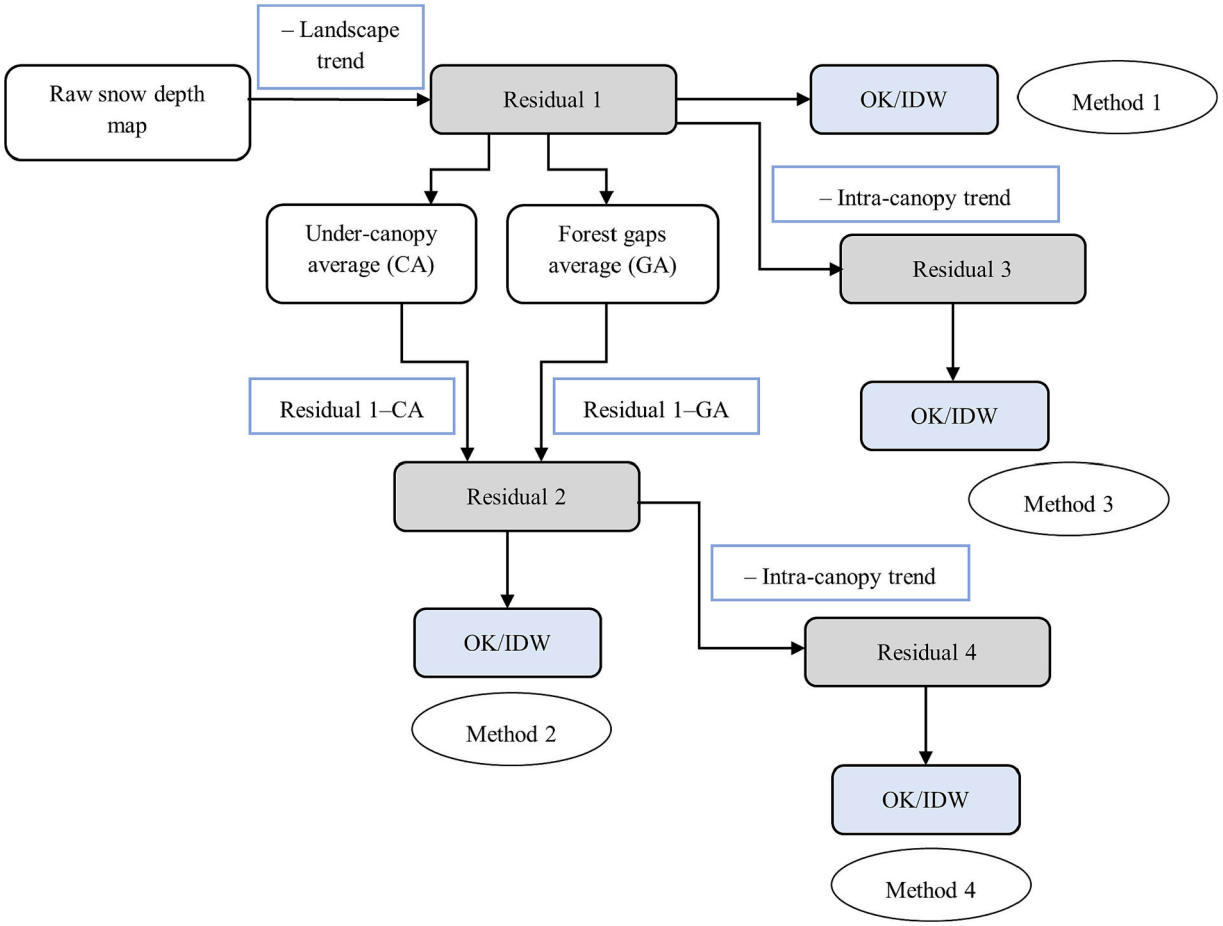

Fig. 4. Schematic illustration of the interpolation methods.

residuals ('residual 2' in Fig. 4). This operation thus removes the potentially systematic positive bias in gaps relative to canopies. Then, the 2nd-level residuals were spatially interpolated with OK and IDW. The landscape trend and the canopy vs. gap trends are then added back to the interpolated residuals to obtain the estimated snow depths in unsampled areas.

3.3.3. *Interpolation method 3*

In method 3, the detrended snow depth data from method 1 (residual 1) was used to determine the intra-canopy snow depth patterns. A number of studies reported increasing snow depths with increased distance from tree stems towards the tree canopy (Pomeroy and Dion, 1996; Musselman et al., 2008; Revuelto et al., 2015; Zheng et al., 2019). As such, the correlation between snow depth under the canopy and the scaled distance from the tree stem was investigated. For each snow depth grid cell located within a canopy, the distance from the tree stem location (as identified by treetops) to the snow depth grid cell was calculated and then scaled by the total distance from the tree stem to the tree canopy edge. A scaled distance was used to account for the different tree canopy sizes. Then, a second-order polynomial function was fitted to snow depth residual 1 and corresponding scaled distances (Fig. 5) to estimate the intra-canopy trend (Table 1; Eq. 4). Since the point density tended to increase from the tree stem towards the canopy edges, the polynomial model was weighed according to point density over the scaled distance. The point density was estimated with a gaussian kernel window with a 0.1 scaled distance bandwidth (standard deviation = 0.1). An interaction term with tree height was included, to account for the different intra-canopy trends with tree sizes (Fig. 5). The fitted polynomial function showed an adjusted R^2 of 0.70. Finally, the intra-canopy trend was removed from residual 1, and the residuals from the

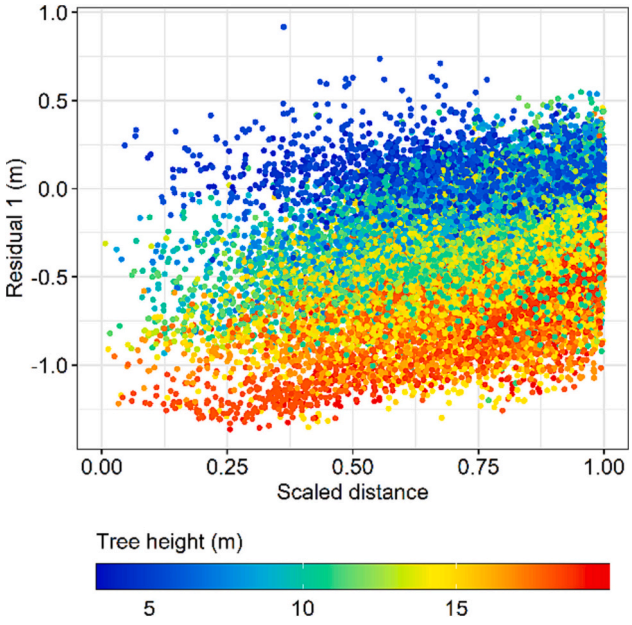

Fig. 5. Variation of snow depth residual 1 with scaled distance. Points are colored by the tree height.

intra-canopy trend ('residual 3' in Fig. 4) were spatially interpolated using OK and IDW (Fig. 4).

3.3.4. Interpolation method 4

Method 4 removed both the landscape trend and the canopy vs. gap trend (yielding the 2nd order residuals in Fig. 4). The same intra-canopy polynomial model described in method 3 was fitted on the 2nd order residuals to obtain the intra-canopy trend (Fig. 4 and Table 1; Eq. 4), yielding an adjusted R^2 of 0.70. Subtracting the intra-canopy trend from residual 2 yielded the 4th-level residuals ('residual 4' in Fig. 4), which were then spatially interpolated using OK and IDW.

3.4. Cross-validation of the interpolation methods

Cross-validation was used to estimate the prediction performance of the respective interpolation methods. One-hundred random snow depth grid cells were used as test data from the entire study area. The effect of the distance between the sampled and unsampled grid cells on the prediction (i.e., the effect of the local point density on the quality of the interpolation) was investigated in the following manner. All the surrounding training (sampled) grid cells within a distance D of each of the test (unsampled) grid cells were removed from the training set. Then, the models were trained on training data that are beyond the distance D from test data (Fig. 6) and these trained models were used to predict the snow depths at test locations. D varied from 0 to 5 m, with an interval of 0.5 m. The whole procedure was repeated 20 times to reduce the sampling uncertainty. The root mean squared error (RMSE), bias, and Pearson correlation coefficient were used as validation statistics and reported as a function of the mean distance between the unsampled (test) grid cells and the three closest training grid cells to each test grid cell. The validation statistics were calculated for the four interpolation methods as well as for the trend models only, i.e., without spatial interpolation of the trend residuals, and compared with the reference method (spatial interpolation of raw snow depths using OK and IDW) to investigate the effect of incorporating trends in snow depth estimates.

4. Results and discussion

4.1. Interpolated snow depth maps

Fig. 7 shows the interpolated snow depth obtained by the different methods. Since snow depth maps derived from the OK method showed negligible to no visible difference with the corresponding IDW snow depth estimates, only the results from OK are shown in the main text. IDW results are included in supplementary. The snow depth patterns obtained by the four interpolation methods are overall similar, but fine scale differences are apparent (Fig. 7a–d). For instance, the area west of the large gap is covered by a dense canopy (Fig. 3) and consequently shows more observation gaps due to few lidar returns in this area (Fig. 1c, d). The snow depths interpolated by method 1 in this area display smoothed spatial variability, notably between under-canopy and forest gaps (Fig. 7a). Consideration of the measured canopy vs. gap snow depth trend in method 2 shows some disruptions in the previously smoothed snow depth variability in this area, i.e., snow depth differences between under-canopy areas and forest gaps (Fig. 7b). Compared to methods 1 and 2, the consideration of intra-canopy snow depth trend in methods 3 and 4 shows clear differences in snow depths between under-canopy areas and forest gaps and snow depth variability under the canopy (Fig. 7c, d). Snow depth maps produced by methods 3 and 4 do not exhibit any visual difference, implying that it is rather the intra-canopy trend that causes most of the differences in snow depths between under-canopy and forest gaps, i.e., consideration of the canopy vs. gap trend in method 4, in addition to the other systematic trends considered in method 3, does not seem to produce visibly different results compared to method 3.

Snow depth differences between methods illustrate the relative effect of the different interpolation methods (Fig. 7 -bottom row). Negligible differences in snow depths between method 1 and the reference method (Fig. 7e) indicate that the landscape trend is not pronounced in the data. The larger snow depth differences between methods 2 and 1 (Fig. 7f) show the substantial impact of including the canopy vs. gap snow depth trend. Fig. 7g shows comparatively large differences in snow depths between methods 3 and 1 and adding the intra-canopy trend on residual 1 tends to smooth the sharper gap vs. canopy pattern introduced by method 2. It further suggests that method 1 overestimates snow depths at some locations (negative values in Fig. 7g) and underestimates (positive values in Fig. 7g) at others compared to method 3. Similar patterns are observed in Fig. 7h, which shows the effect of adding the intra-canopy trend on residual 2.

The different interpolation methods resulted in different probability density distributions of snow depths over the study area (Fig. 8). The higher raw snow depth observed in forest gaps compared to under-canopy in Fig. 8 corroborates results found in previous studies (Musselman et al., 2008; Revuelto et al., 2015; Uhlmann et al., 2018; Mazzotti et al., 2019). This difference becomes more evident once the snow depths are interpolated, as the snow depth probability density distributions below the canopy become more skewed towards smaller values. The snow depth probability density distribution in full domain obtained using the raw (not interpolated) data appears to be biased by the higher snow depths in forest gaps. This is not surprising due to the over-sampling and under-sampling of snow depths in forest gaps and under-canopy, respectively (see snow depth map in Fig. 1). All the interpolated methods implemented here seem to rectify this issue. Moreover, the similar probability density distributions of snow depths in forest gaps obtained by all the interpolation methods indicate that these have the least effect in the forest gaps, where the point density is highest, than in the forest. In canopies, reference (spatial interpolation of raw snow depths using OK), methods 1 and 2 show noisier and tighter (less variable) distributions, whereas methods 3 and 4 show similar, smoother, and wider (more variable) distributions. These results show that estimating area-wide snow depth distributions and their summary statistics from sparse lidar snow depths in forested areas entails a significant error and interpolation is necessary to eliminate the bias due to canopy under-sampling.

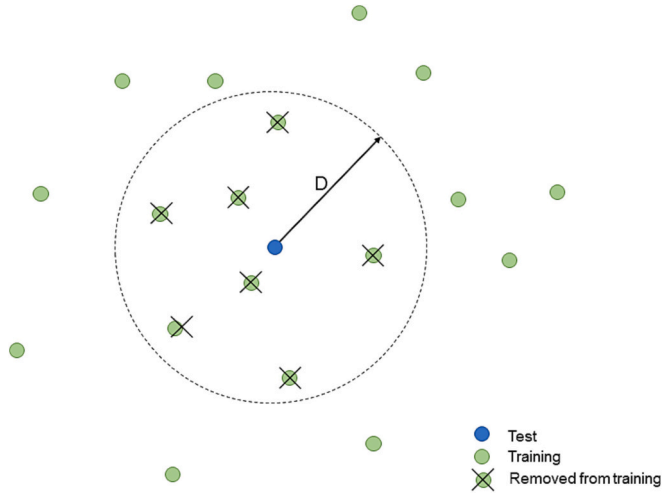

Fig. 6. Illustration of the cross-validation scheme. Selected test grid cells (blue) are chosen randomly and training grid cells within a separation distance (D) are eliminated to investigate the impact of lidar sampling density on the interpolation performance. (For interpretation of the references to colour in this figure legend, the reader is referred to the web version of this article.)

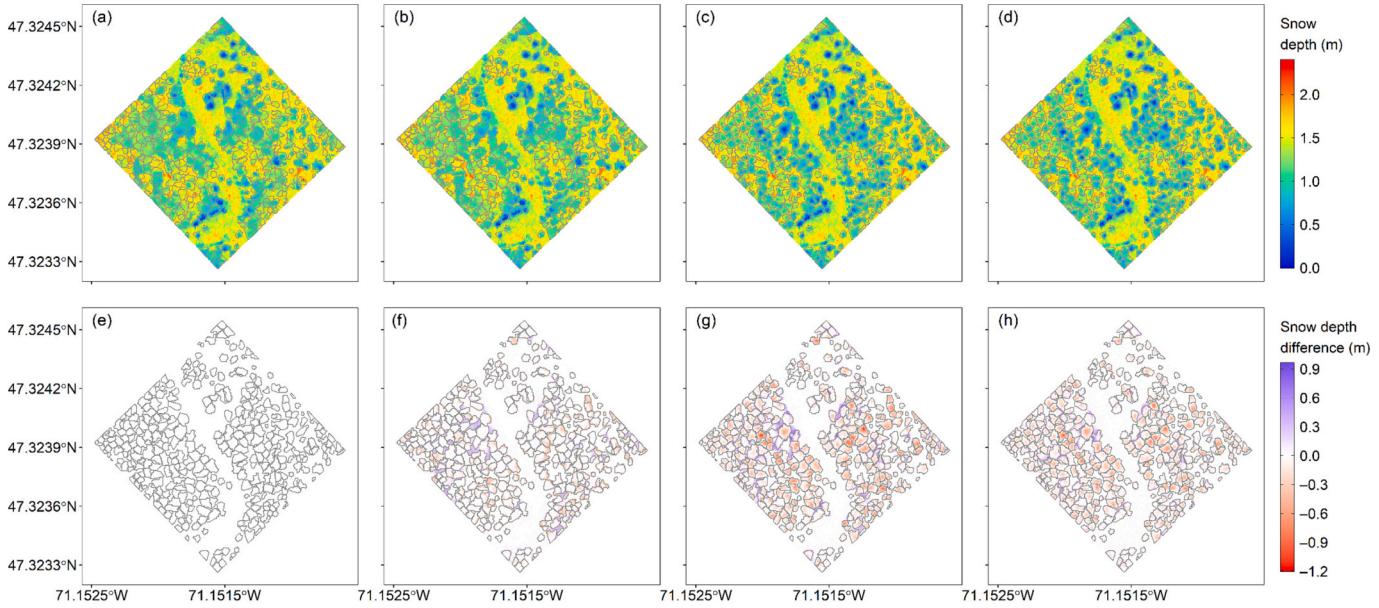

Fig. 7. Interpolated snow depth maps: (a) method 1, (b) method 2, (c) method 3, (d) method 4; snow depth difference between methods: (e) method 1 – reference, (f) method 2 – method 1, (g) method 3 – method 1, and (h) method 4 – method 2. Canopy polygons are demarcated by grey lines. Note that Fig. 7e shows as white due to the very small snow depth differences (−0.02–0.03 m).

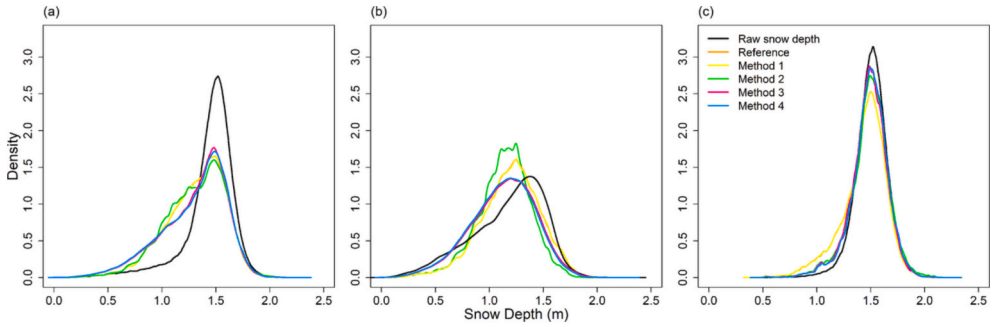

Fig. 8. Probability density distributions of snow depths interpolated by OK for (a) full domain, (b) under-canopy, and (c) forest gaps. The density distributions were computed using a gaussian kernel with a standard deviation of 0.01. The Raw snow depth distributions correspond to snow depths not interpolated (See section 3.1).

4.2. Cross-validation

Of all the methods with spatial interpolation (trends + spatial interpolation of residuals; column one in Fig. 9), method 1 shows the lowest interpolation performance with higher RMSE, bias, and lower correlation coefficient. Moreover, method 1 exhibits negligible differences with the reference method in which spatial interpolation techniques were directly applied to the raw snow depths (black vs pink graphs in Fig. 9a, c, e). This suggests an absence of pronounced landscape trend in the study area; hence, removing or not the trend does not have a substantial effect on interpolation. However, in larger areas and/or with more pronounced elevation ranges where temperature and precipitation lapse rate gradients start to impact snow accumulation, the landscape trend would be expected to be important and would need to be considered. Among the four methods, method 4 shows the highest performance with lower RMSE, bias, and higher correlation coefficient. Methods 3 and 2 scored second and third in terms of RMSE and correlation coefficient, though showing similar biases (Fig. 9c). The OK and IDW spatial interpolation techniques generally yield similar accuracies (Supplement Fig. S3). All methods show degrading accuracies with increasing distance between unsampled and sampled snow depth grid cells.

Column two in Fig. 9 shows the prediction error when using only the systematic trends, without spatial interpolation of residuals, and allows seeing the effect of incorporating trends within the interpolation methods. Similar to when using spatial interpolation (Fig. 9, column one), methods 1 and 4 show the lowest and highest performances respectively, while methods 3 and 2 show intermediate performances. However, the noticeable bias in method 3 seen in Fig. 9d indicates that ignoring the canopy vs. gap trend in method 3 may lead to a positive bias in mean snow depth across the domain, due to lidar snow depth being biased towards the gaps (Fig. 1 and 8). However, the spatial interpolation of residuals in method 3 seems to largely compensate this problem, as the bias becomes comparable, albeit slightly larger, than method 2 and 4 which both include the gap vs. canopy trend (Fig. 9c). In general, column two shows that incorporating trends within the interpolation methods slows the degradation of the prediction accuracy with increasing distance between unsampled and sampled points.

4.2.1. Impact of lidar snow depth sampling density on interpolation

Fig. 9 also provides an indication of two limiting distances (or sampling densities) within which the interpolation methods can be used. As observed from the first column, up to a distance of ~1 m between sampled and unsampled locations, all methods show similar and better performances compared to when the inter-grid separation distances increase by >1 m. This suggests that when the distance between

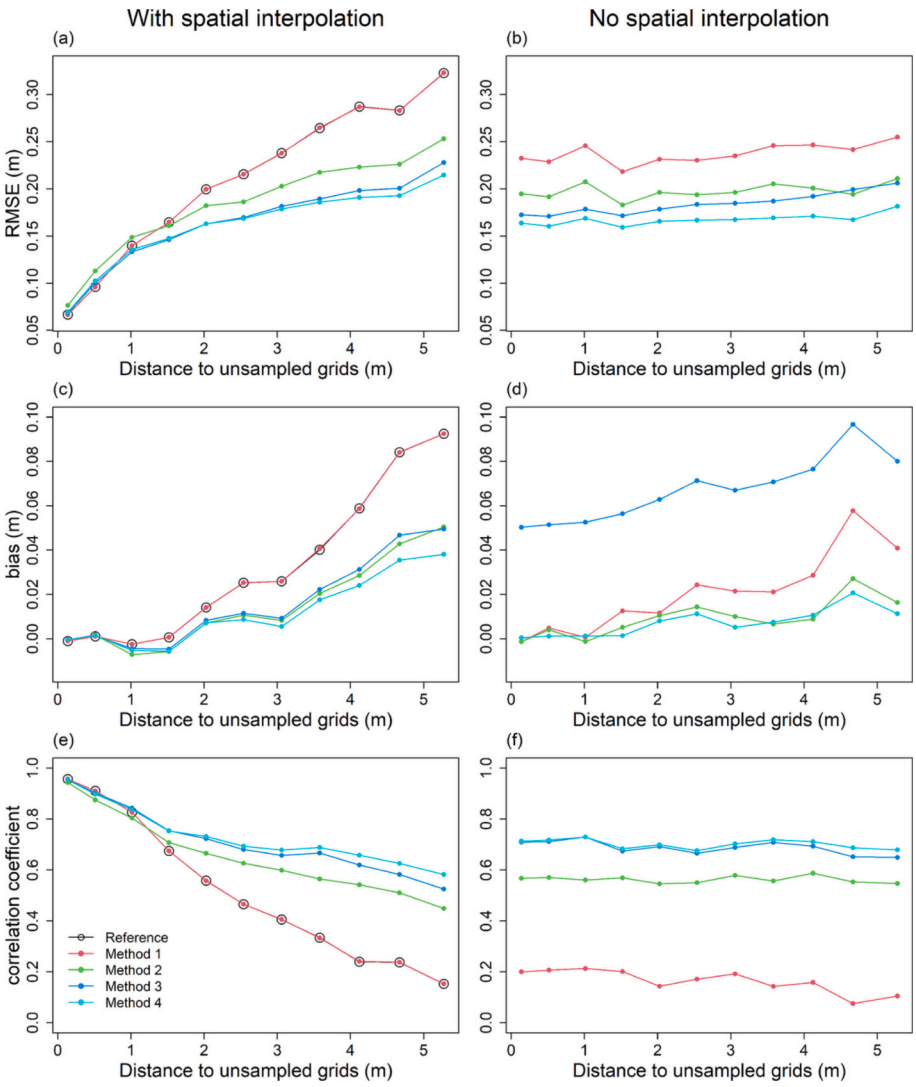

Fig. 9. Error statistics with the distance between unsampled (test) and sampled (training) grid cells (a, b) RMSE (c, d) bias, and (e, f) correlation coefficient. Panels in the first column are for methods with spatial interpolation. Reference indicates spatial interpolation of raw snow depths with OK, without consideration of trends. The second column is without spatial interpolation, i.e., only using trends for prediction of the unsampled grid cells.

unsampled and sampled grid cells is <1 m, (i.e., ground surface lidar point density is >1 pt. m^{-2}) spatial interpolation techniques based on spatial autocorrelation like OK have sufficient information to resolve and reconstruct small-scale snow depth patterns. Above 1 m, the performance of the different methods is no longer similar and starts degrading, but at a slower rate than that below 1 m. Column one shows that past 1 m, incorporating trends slows the degradation of accuracies with increasing inter-grid cell distances, and canopy vs. gap and intra-canopy trends (method 2, 3, and 4) significantly improve the interpolation performances compared to the reference method that ignores these trends. This highlights the necessity of explicitly modelling trends past this distance as they are not well represented by OK interpolation when the inter-grid cell distance increases beyond 1 m (lidar ground point density is <1 pt. m^{-2}).

A comparison of the two columns in Fig. 9 suggests another limiting distance at ~2.5–3 m. Past this distance, the interpolation of trend residuals with OK (Fig. 9 a, c, e) degrades the performance compared to using the trends alone for prediction (Fig. 9 b, d, f). This is particularly evident in the RMSE and correlation coefficient plots. This suggests that when the distance between sampled and unsampled grid cells is larger than 2.5–3 m (point density <0.33–0.40 pt. m^{-2}), the snow depth grid cells are too separated to inform each other, i.e., to provide meaningful interpolation based on spatial autocorrelation. The resulting interpolated snow depth maps thus suffer from high uncertainties. As such, when the ground surface point density is lower, the modelled systematic trends (landscape, canopy vs. gap, and intra-canopy) would provide more accurate gap-filled snow depth maps than using spatial interpolation methods.

4.2.2. *Comparison to previous studies*

The first, lower limiting distance found in this study (1 m, or ground point density of 1 pt. m^{-2}) is in agreement with the threshold ground surface point density found by Guo et al. (2010) and Zheng et al. (2019) for airborne lidar surveys in order to generate high-accuracy DEMs and to capture the tree wells in snow surfaces. Similar to Guo et al. (2010), we found an RMSE of <0.15 m for interpolated snow depths when ground surface point density is larger than 1 pt. m^{-2}. However, Zheng et al. (2019) emphasized that the effect of point density is more significant in densely forested areas like Montmorency than in more sparsely forested areas, as with latter, low lidar point density can offset the overestimation in tree wells under canopies and underestimation at snow peaks in forest gaps.

The second, higher limiting distance of 2.5–3 m is in the same order of magnitude as the maximum canopy radius (7 m) found in

Montmorency, and half of the scale break distance (4.5 m in bare earth topography+trees and 6.5 m in snow depth) found for Montmorency by Dharmadasa et al. (2023). Therefore, when the distance between sampled and unsampled grid cells is larger than this threshold, we risk interpolating grid cells with little to no spatial correlation (i.e., grid cells within and outside the canopy), hence degrading the accuracy of gap-filling. Especially beneath the canopy, intra-canopy trends help preserving the variability of snow depths when ground point density is lower. This confirms our hypothesis that spatial interpolation methods that only exploit the spatial correlation of available lidar snow depths will be insufficient to fill the gaps in coniferous forests, where systematic variations in snow depth occur over beneath and among tree canopies.

5. Conclusions

Given the typical under-sampling of lidar ground surface points under the canopy and limitation of existing interpolation techniques in accurately representing snow depth variability within canopy areas, the new interpolation methods introduced in this study exhibit promising potential. Our results suggest that the spatial interpolation method that incorporates systematic trends in snow accumulation at the landscape, canopy vs. gaps, and intra-canopy scales yield significant improvements for gap-filling when the distance between sampled and unsampled lidar snow depth grid cells is larger than 1 m (ground point density of <1 pt. m^{-2}). However, beyond a distance of 2.5–3 m (point density $<$ 0.33–0.40 pt. m^{-2}), the point separation becomes larger than the snow depth spatial correlation scale, and spatial interpolation based on proximity alone becomes useless. Below a separation distance of 1 m, (i.e., ground surface point density $>$ 1 pt. m^{-2}), spatial interpolation methods without consideration of trends are sufficient to capture and reconstruct the small-scale variability of snow depths. This suggests that consideration of the trends only becomes useful for areas with a ground surface point density of <1 pt. m^{-2}. Within these limiting distances, consideration of trends along with spatial interpolation techniques can resolve the small-scale variability and thereby reduce the likely overestimation of snow depths under the canopy. In this context, within the prescribed distance range, method 4, which includes all systematics trends yielded the best performance followed by methods 3, 2, and 1, respectively.

6. Recommendations

The proposed interpolation method in this study can be easily applied to any area subjected to fine-tuning of the window size for treetop identification. While this approach primarily targets coniferous environments, its adaptability to deciduous settings is plausible. However, given the limited intra-canopy and canopy vs. gap snow depth variations in deciduous environments, modelling these trends as part of the interpolation scheme may not yield significant improvements. It is worth noting that running the R script (Supplement) on a standard computer can be somewhat computationally intensive. For instance, on a Core i7 computer equipped with 32 Gb RAM and a 3.2 GHz processor, the R script took approximately 1.5 h to execute (excluding the cross-validation part) for a 100 $\times$ 100 m area. In contrast, on a Core i7 computer with 64 Gb RAM and a 3.6 GHz processor, the same took 0.7 h to complete. Therefore, we expect that the computational demand of the method will be lower when implemented on a high-performance computing system. It is also expected that the areas larger than the study site tested here would cause increased computational time.

Author contributions

Conceptualization, C.K.; methodology, C.K. and V.D.; formal analysis, V.D. and C.K.; data curation, V.D.; writing-original draft preparation, V.D.; writing-review and editing, C.K. and M.B.; supervision, C.K. and M.B.; project administration, C.K.; funding acquisition, C.K.

Funding

This study was financially supported by the Canada Research Chair program (grant number 231380) and the Natural Sciences and Engineering Research Council of Canada (NSERC discovery grant CRSNG-RGPIN-2015-03844) (Christophe Kinnard) and a doctoral scholarship from the Centre de Recherche sur les Interactions Bassins Versants-Écosytèmes Aquatiques (RIVE, Vasana Dharmadasa).

CRediT authorship contribution statement

Vasana Dharmadasa: Writing – original draft, Methodology, Formal analysis, Data curation. **Christophe Kinnard:** Writing – review & editing, Supervision, Project administration, Methodology, Funding acquisition, Formal analysis, Conceptualization. **Michel Baraër:** Writing – review & editing, Supervision.

Declaration of competing interest

The authors declare no conflict of interest.

Data availability

The data presented in this study are available on a reasonable request from the corresponding author.

Acknowledgments

The authors extend their appreciation to the members of GlacioLab for their help during fieldworks.

Appendix A. Supplementary data

Supplementary data to this article can be found online at https://doi.org/10.1016/j.coldregions.2024.104134.

References

Blue Marble Geographics, 2020. Global Mapper. Retrieved from Hallowell, ME, USA: www.bluemarblegeo.com/knowledgebase/global-mapper.

Broxton, P.D., Harpold, A.A., Biederman, J.A., Troch, P.A., Molotch, N.P., Brooks, P.D., 2015. Quantifying the effects of vegetation structure on snow accumulation and ablation in mixed-conifer forests. Ecohydrology 8, 1073–1094. https://doi.org/10.1002/eco.1565.

Burrough, P.A., 1986. Principles of geographical information systems for land resources assessment. Geocarto Int. 1 (3), 54. https://doi.org/10.1080/10106048609354060.

Currier, W.R., Lundquist, J.D., 2018. Snow depth variability at the forest edge in multiple climates in the western United States. Water Resour. Res. 54 (11), 8756–8773. https://doi.org/10.1029/2018WR022553.

Dalponte, M., Coomes, D.A., 2016. Tree-centric mapping of forest carbon density from airborne laser scanning and hyperspectral data. Methods Ecol. Evol. 7 (10), 1236–1245. https://doi.org/10.1111/2041-210X.12575.

Deems, J.S., Painter, T.H., Finnegan, D.C., 2013. Lidar measurement of snow depth: a review. J. Glaciol. 59 (215), 467–479. https://doi.org/10.3189/2013JoG12J154.

Dharmadasa, V., Kinnard, C., Baraër, M., 2022. An accuracy assessment of snow depth measurements in agro-forested environments by UAV lidar. Remote Sens. 14 (7), 1649. https://doi.org/10.3390/rs14071649.

Dharmadasa, V., Kinnard, C., Baraër, M., 2023. Topographic and vegetation controls of the spatial distribution of snow depth in agro-forested environments by UAV lidar. Cryosphere 17 (3), 1225–1246. https://doi.org/10.5194/tc-17-1225-2023.

Erxleben, J., Elder, K., Davis, R., 2002. Comparison of spatial interpolation methods for estimating snow distribution in the Colorado Rocky Mountains. Hydrol. Process. 16, 3627–3649. https://doi.org/10.1002/hyp.1239.

Geodetics Inc, 2019. LiDARTool™ User Manual (Document 20149 Rev I). Retrieved from San Diego, CA, USA: https://geodetics.com/.

Glira, P., Pfeifer, N., Mandlburger, G., 2016. Rigorous strip adjustment of UAV-based laserscanning data including time-dependent correction of trajectory errors. Photogramm. Eng. Remote. Sens. 82, 945–954. https://doi.org/10.14358/PERS.82.12.945.

Guo, Q., Li, W., Yu, H., Alvarez, O., 2010. Effects of topographic variability and lidar sampling density on several DEM interpolation methods. Photogramm. Eng. Remote. Sens. 76 (6), 701–712. https://doi.org/10.14358/PERS.76.6.701.

Harder, P., Pomeroy, J., Helgason, W., 2020. Improving sub-canopy snow depth mapping with unmanned aerial vehicles: Lidar versus structure-from-motion techniques. Cryosphere 14, 1919–1935. https://doi.org/10.5194/tc-14-1919-2020.

Harpold, A.A., Guo, Q., Molotch, N., Brooks, P.D., Bales, R., Fernandez-Diaz, J.C., et al., 2014. Lidar-derived snowpack data sets from mixed conifer forests across the Western United States. Water Resour. Res. 50, 2749–2755. https://doi.org/10.1002/2013WR013935.

Hojatimalekshah, A., Uhlmann, Z., Glenn, N., Hiemstra, C., Tennant, C., Graham, J., et al., 2021. Tree canopy and snow depth relationships at fine scales with terrestrial laser scanning. Cryosphere 15, 2187–2209. https://doi.org/10.5194/tc-15-2187-2021.

Hopkinson, C., Sitar, M., Chasmer, L., Treitz, P., 2004. Mapping snowpack depth beneath forest canopies using airborne lidar. Photogramm. Eng. Remote. Sens. 70 (3), 323–330.

Hopkinson, C., Collins, T., Anderson, A., Pomeroy, J., Spooner, I., 2012a. Spatial snow depth assessment using lidar transect samples and public GIS data layers in the Elbow River watershed, Alberta. Can. Water Resourc. J. 37 (2), 69–87. https://doi.org/10.4296/cwrj3702893.

Hopkinson, C., Pomeroy, J., Debeer, C., Ellis, C., Anderson, A., 2012b. *Relationships between snowpack depth and primary lidar point cloud derivatives in a mountainous environment.* Paper presented at the Remote Sensing and Hydrology, Jackson Hole, Wyoming, USA, 27–30 September 2010.

Isaaks, E.H., Srivastava, R.M., 1989. Applied Geostatistics. Oxford University Press.

Jacobs, J.M., Hunsaker, A.G., Sullivan, F.B., Palace, M., Burakowski, E.A., Herrick, C., et al., 2021. Snow depth mapping with unpiloted aerial system lidar observations: a case study in Durham, New Hampshire, United States. Cryosphere 15 (3), 1485–1500. https://doi.org/10.5194/tc-15-1485-2021.

Jost, G., Weiler, M., Gluns, D.R., Alila, Y., 2007. The influence of forest and topography on snow accumulation and melt at the watershed-scale. J. Hydrol. 347, 101–115. https://doi.org/10.1016/j.jhydrol.2007.09.006.

Koutantou, K., Mazzotti, G., Brunner, P., Webster, C., Jonas, T., 2022. Exploring snow distribution dynamics in steep forested slopes with UAV-borne LiDAR. Cold Reg. Sci. Technol. 200, 103587 https://doi.org/10.1016/j.coldregions.2022.103587.

Lehning, M., Grünewald, T., Schirmer, M., 2011. Mountain snow distribution governed by an altitudinal gradient and terrain roughness. Geophys. Res. Lett. 38, L19504. https://doi.org/10.1029/2011GL048927.

López-Moreno, J.I., Latron, J., Lehmann, A., 2010. Effects of sample and grid size on the accuracy and stability of regression-based snow interpolation methods. Hydrol. Process. 24 (14), 1914–1928. https://doi.org/10.1002/hyp.7564.

Mazzotti, G., Currier, W., Deems, J.S., Pflug, J.M., Lundquist, J.D., Jonas, T., 2019. Revisiting snow cover variability and canopy structure within forest stands: Insights from airborne lidar data. Water Resour. Res. 55, 6198–6216. https://doi.org/10.1029/2019WR024898.

Michele, C., Avanzi, F., Passoni, D., Barzaghi, R., Pinto, L., Dosso, P., et al., 2016. Using a fixed-wing UAS to map snow depth distribution: an evaluation at peak accumulation. Cryosphere 10, 511–522. https://doi.org/10.5194/tc-10-511-2016.

Morsdorf, F., Kötz, B., Meier, E., Itten, K.I., Allgöwer, B., 2006. Estimation of LAI and fractional cover from small footprint airborne laser scanning data based on gap fraction. Remote Sens. Environ. 104, 50–61. https://doi.org/10.1016/j.rse.2006.04.019.

Musselman, K.N., Molotch, N.P., Brooks, P.D., 2008. Effects of vegetation on snow accumulation and ablation in a mid-latitude sub-alpine forest. Hydrol. Process. 22 (15), 2767–2776. https://doi.org/10.1002/hyp.7050.

Painter, T., Berisford, D., Boardman, J., Bormann, K.J., Deems, J., Gehrke, F., et al., 2016. The Airborne Snow Observatory: Fusion of scanning lidar, imaging spectrometer, and physically-based modeling for mapping snow water equivalent and snow albedo. Remote Sens. Environ. 184, 139–152. https://doi.org/10.1016/j.rse.2016.06.018.

Pajares, G., 2015. Overview and current status of remote sensing applications based on Unmanned Aerial Vehicles (UAVs). Photogramm. Eng. Remote. Sens. 81, 281–329. https://doi.org/10.14358/PERS.81.4.281.

Pomeroy, J.W., Dion, K., 1996. Winter radiation extinction and reflection in a boreal pine canopy: measurements and modelling. Hydrol. Process. 10, 1591–1608.

Revuelto, J., López-Moreno, J., Azorin-Molina, C., Vicente-Serrano, S.M., 2014. Topographic control of snowpack distribution in a small catchment in the central Spanish Pyrenees: Intra- and inter-annual persistence. Cryosphere 8, 1989–2006. https://doi.org/10.5194/tc-8-1989-2014.

Revuelto, J., López-Moreno, J., Azorin-Molina, C., Vicente-Serrano, S.M., 2015. Canopy influence on snow depth distribution in a pine stand determined from terrestrial laser data. Water Resour. Res. 51, 3476–3489. https://doi.org/10.1002/2014WR016496.

Roussel, J.-R., Auty, D., Coops, N.C., Tompalski, P., Goodbody, T.R.H., Meador, A.S., et al., 2020. lidR: an R package for analysis of Airborne Laser Scanning (ALS) data. Remote Sens. Environ. 251, 112061 https://doi.org/10.1016/j.rse.2020.112061.

Roussel, J.-R., Auty, D., Boissieu, F.D., Meador, A.S., Jean-François, B., Demetrios, G., et al., 2022. Airborne LiDAR data manipulation and visualization for forestry applications. R package version 4.0.2. Retrieved from. https://cran.r-project.org/package=lidR.

Tinkham, W.T., Smith, A.M.S., Marshall, H., Link, T., Falkowski, M., Winstral, A., 2014. Quantifying spatial distribution of snow depth errors from lidar using random forest. Remote Sens. Environ. 141, 105–115. https://doi.org/10.1016/j.rse.2013.10.021.

Uhlmann, Z., Glenn, N.F., Spaete, L.P., Hiemstra, C., Tennant, C., McNamara, J., 2018. *Resolving the influence of forest-canopy structure on snow depth distributions with terrestrial laser scanning.* Paper presented at the IGARSS 2018–2018 IEEE International Geoscience and Remote Sensing Symposium, Valencia, Spain, 22–27 July 2018.

Varhola, A.S., Coops, N.C., Bater, C.W., Teti, P., Boon, S., Weiler, M., 2010. The influence of ground- and lidar-derived forest structure metrics on snow accumulation and ablation in disturbed forests. Can. J. For. Res. 40, 812–821. https://doi.org/10.1139/X10-008.

VelodyneLiDAR, 2018. VLP-16 User Manual. Retrieved from San Jose, USA: https://www.velodynelidar.com.

Venables, W.N., Ripley, B.D., 2002. Modern Applied Statistics with S, Fourth edition. Springer, New York.

Winstral, A., Elder, K., Davis, R.E., 2002. Spatial snow modeling of wind-redistributed snow using terrain-based parameters. J. Hydrometeorol. 3 (5), 524–538. https://doi.org/10.1175/1525-7541(2002)003<0524:Ssmowr>2.0.Co;2.

Zheng, Z., Kirchner, P.B., Bales, R.C., 2016. Topographic and vegetation effects on snow accumulation in the southern Sierra Nevada: a statistical summary from lidar data. Cryosphere 10, 257–269. https://doi.org/10.5194/tc-10-257-2016.

Zheng, Z., Ma, Q., Qian, K., Bales, R.C., 2018. Canopy effects on snow accumulation: observations from lidar, canonical-view photos, and continuous ground measurements from sensor networks. Remote Sens. 10, 1769. https://doi.org/10.3390/rs10111769.

Zheng, Z., Ma, Q., Jin, S., Su, Y., Guo, Q., Bales, R.C., 2019. Canopy and terrain interactions affecting snowpack spatial patterns in the Sierra Nevada of California. Water Resour. Res. 55 (11), 8721–8739. https://doi.org/10.1029/2018wr023758.